05

Specific features of the thermoelectric characteristics for 1D free-standing and epitaxial structures formed on transition metals

© S.Yu. Davydov

Ioffe Institute,
St. Petersburg, Russia

E-mail: sergei_davydov@mail.ru

Received February 1, 2024
Revised February 1, 2024
Accepted March 25, 2024

Analytical expressions for dispersion, effective masses of carriers, and densities of states for the free cumulene, polyyne, and 1D structures AB, AB2, and ABC are obtained in the tight tight-binding approximation by the Green's function method. It is demonstrated that the densities of states of all considered structures are characterized by root divergences as the chemical potential approaches the boundaries of the continuous spectrum of these structures. The experimental and theoretical prerequisites for the possibility of fabrication long carbon chains on the grooved faces of *d*-metals are discussed. The influence of the substrate on the spectral characteristics and density of states of one-dimensional structures is estimated. Assuming the conductivity of these structures to be diffusive, expressions for the Seebeck coefficient and the thermoelectric power factor are obtained for two variants of the scattering time approximation in the Boltzmann equa-tion. The experimental and theoretical prerequisites for the possibility of formation long carbon chains on the grooved faces of d-metals are discussed. The influence of the substrate on the spectral characteristics and density of states of one-dimensional struc-tures is estimated.

Keywords: cumulene, polyyne, 1D structures AB, AB_2, ABC, Seebeck coefficient, thermoelectric power factor.

DOI: 10.61011/PSS.2024.05.58500.16

1. Introduction

With the advent of graphene [1] vigorous search for other 2D compounds started: „libraries" [2.3], databases [4–6], roadmap [7], atlases of such materials were prepared [8]. Interest, though much lower, was also shown in 1D structures. Primarily, focus on carbyne, that had been already studied for half a century (see [9]), was certainly enhanced. Carbyne is a one-dimensional chain of carbon atoms. Two types of carbynes are distinguished: double-bonded metallic cumulene (...=C=C=...) and semiconducting polyyne with alternating single and triple bonds (... ≡C−C≡C−C≡ ...) [10–17]. Theoretically expected strength, modulus of elasticity and hardness of carbynes are higher than those of any other known material, including diamonds, carbon nanotubes and graphene, therefore, new composite materials may be created. Another actually unexamined application includes the achievement of maximum channel width limit (thickness equal to one carbon atom) for field transistors. Besides strength properties, conductance of carbynes was of great interest (see 2.2).

AB compounds IV−IV, III−V and II−VI [18–22] and metals appeared to be the next [23,24]. Applications of 1D materials are discussed in [23–30] (note that nanoribbons and nanotubes are not addressed herein). Besides carbynes, AB, AB_2 and ABC structures are discussed herein. The last two structures that, strictly speaking, should be referred to as quasi-one-dimensional have been chosen according to the conclusions in [31,32] which showed theoretically that AB_2 and ABC had the highest percentage among triatomic 2D compounds.

This study investigates thermoelectric (TE) properties of 1D structures, that, as far as known, have received almost no attention: an exception is [33] that investigated hopping conductivity of carbynes at high pressures and temperatures. This situation seems strange because a considerable amount of literature (see [34,35] and [36–38]) has been published on the study of TE properties of 2D compounds. The Seebeck coefficient S and thermoelectric power factor $PF = \sigma S^2$ of free 1D structures will be studied as TE properties, where σ is conductivity, and potential generation of 1D structures on striated faces of transition metals will be discussed.

2. Free-standing 1D structures

2.1. Electronic spectrum

Let us start from ABC structure shown in Figure 1 that may be treated as an AB chain decorated with atoms C. Let us introduce atom Green's functions

$$g_{a,b,c} = (\omega - \varepsilon_{a,b,c} + i0^+)^{-1} \quad (1)$$

respectively, for atoms A, B and C, where ω is the energy variable, $\varepsilon_{a,b,c}$ are energies of p_z-states of atoms A, B, C. Let us now include π-interactions t and $t_\perp$ between atoms

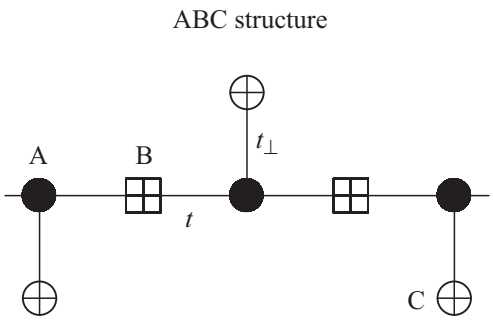

Figure 1. Schematic diagram of ABC structure. t and $t_\perp$ are the integrals of electronic transition between A–B and A–C atoms, respectively (plan view).

A–B and A–C, respectively. Using the Dyson equations, we obtain

$$G_{\mathrm{A0A0}} = g_a + g_a t_\perp G_{\mathrm{C0A0}} + g_a t(G_{\mathrm{B}-1} + G_{\mathrm{B}+1}),$$

$$G_{C0A0} = g_c t_\perp G_{\mathrm{A0A0}}, \;\; G_{\mathrm{B}\pm1} = g_b t G_{\mathrm{A0A0}} + g_b t G_{\mathrm{A}\pm2\mathrm{A0}}, \tag{2}$$

$$G_{\mathrm{CC}} = g_c(1 - 4g_a g_b t^2)/D, \quad G_{\mathrm{AA}} = g_a/D,$$

$$G_{\mathrm{BB}} = g_b(1 - g_a g_c t_\perp^2)/D, \tag{3}$$

where

$$D = 1 - g_a g_c t_\perp^2 - 4g_a g_b t^2 \cos^2(ka)$$

or

$$D = (g_a g_b g_c)^{-1}[\Omega_a \Omega_b \Omega_c - \Omega_b t_\perp^2 - 4\Omega_c t^2 \cos^2(ka)]. \tag{4}$$

Electronic spectrum of the given structures is defined is obtained from equation $D = 0$, or

$$\Omega_a \Omega_b \Omega_c - \Omega_b t_\perp^2 - 4\Omega_c t^2 \cos^2(ka) = 0. \tag{5}$$

Let us now consider the solution of equation (5) for the given structures.

1) AB structure spectrum:

$$t_\perp = 0, \;\; \omega_\pm(k) = \bar{\varepsilon} \pm R(k), \;\; R(k) = \sqrt{\Delta^2 + 4t^2 \cos^2(ka)},$$

where

$$\bar{\varepsilon} = (\varepsilon_a + \varepsilon_b)/2, \;\; \Delta = |\varepsilon_a - \varepsilon_b|/2, \;\; \omega_0 = \varepsilon_c.$$

2) AB_2 structure spectrum:

$$\Omega_b = \Omega_c, \;\; R(k) = \sqrt{\Delta^2 + t_\perp^2 + 4t^2 \cos^2(ka)}.$$

A flat band $\omega_0 = \varepsilon_c = 0$ is noted.

3) For ABC structure, a simple analytical expression for dispersion cannot be given because three electronic bands are the solution of cubic equation. Resulting dispersion laws are shown in Figure 2 for the values listed in the figure captions. It should be noted that energies of p-states of boron atom (as atom A), nitrogen atom (as atom B) and carbon atom (as atom C) taken from Herman–Skillman atomic term table [39] and Mann atomic term table [40] approximately meet the conditions used for the calculations $\varepsilon_a = -\varepsilon_b = \varepsilon$, $\varepsilon_c = 0$ or equation $(\varepsilon_a + \varepsilon_b)/2 = \varepsilon_c$ (see the captions in Figure 2). The same may be said about the atoms in columns III, V (as atoms A, B) and IV (as atom C) that belong to the same row of the periodic system.

For ABC structure when $\varepsilon_c \neq 0$, corrections $\xi_i(ka)$ to spectral branches to a first approximation in ε_c are equal to

$$\xi_i(x) = \varepsilon_c \frac{y_i^2 - (\varepsilon^2 + 4t^2 \cos^2 x)}{3y_i^2 - (\varepsilon^2 + t_\perp^2 + 4t^2 \cos^2 x)} \equiv \varepsilon_c \varphi_i(x),$$

$$\varphi_i(x) = \frac{y_i^2 - 1 - 4\cos^2 x}{3y_i^2 - 2 - 4\cos^2 x}, \tag{6}$$

where $x = ka$, $\varphi_i(ka)$ curves are shown in Figure 2, from which it follows that the maximum values have corrections $\varphi_3(ka)$ for a low-energy band. Consideration of non-zero ε_c does not introduce any qualitative changes into ABC band spectrum. It should be noted that spectra equivalent to that shown in Figure 2 are also specific to adparticle-decorated zigzag edges of graphene [41] and graphene nanoribbons [42], and in all the cases there is a narrow (low-disperse) low-energy branch.

Now proceed to characterization of bands of the given structures. It is easy to show that in the vicinity of the Brillouin zone boundary $k = \pi/2a$, energy band extrema of

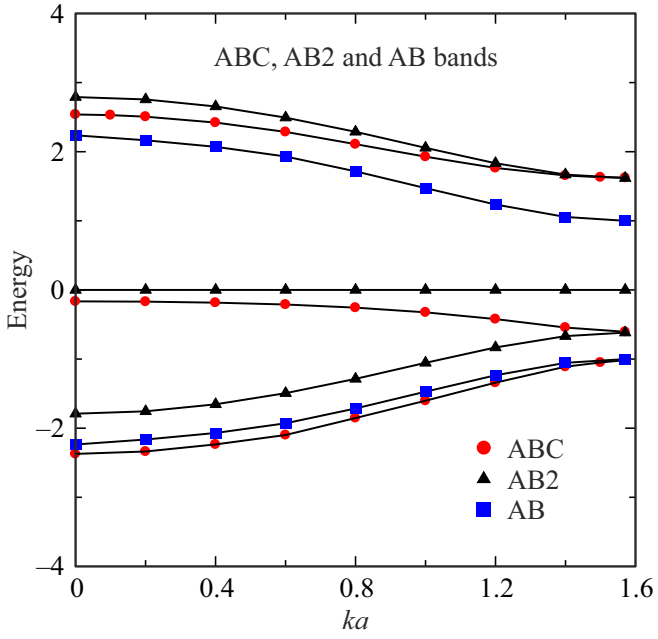

Figure 2. Band spectrum of ABC (circles), AB_2 (triangles) and AB (boxes) structures. Numbers *1* and *2* denote high-energy bands (with positive and negative energies, respectively), number *2* denotes low-energy bands. ABC case: $\varepsilon_a = -\varepsilon_b = \varepsilon$, $\varepsilon = t = t_\perp = 1$, $\varepsilon_c = 0$. AB case: $\varepsilon_a = -\varepsilon_b = \varepsilon$, $\varepsilon = t = 1$, $t_\perp = 0$, $\varepsilon_c = 0$. AB case: $_2$: $\varepsilon_a = \varepsilon$, $\varepsilon_b = \varepsilon_c = 0$, $\varepsilon = t = t_\perp = 1$.

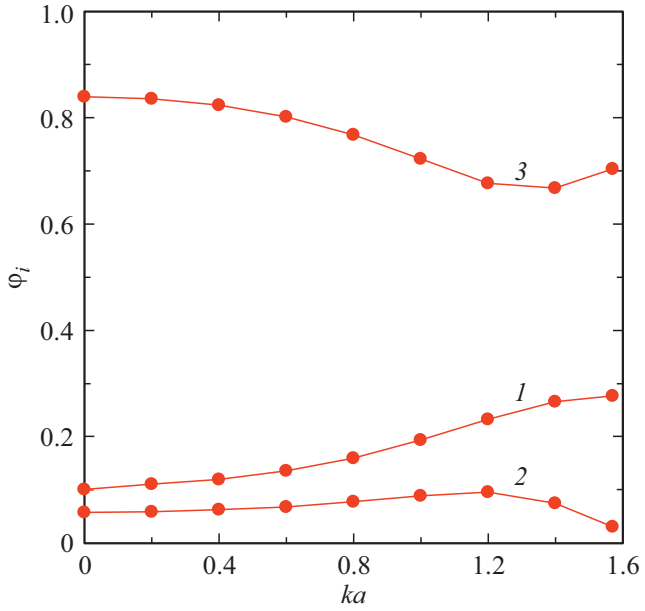

Figure 3. Corrections $\varphi_i(ka)$ (see (7)), where $i = 1, 2, 3$ to bands $i = 1, 2, 3$ for ABC structure (shown in Figure 2) caused by non-zero energy ε_c.

the given structures feature effective masses that are equal to for AB biatomic chain

$$m^1_{\mathrm{AB}} = -m^2_{\mathrm{AB}} = \frac{\hbar^2\Delta}{4t^2a^2},$$

hereinafter numbering of bands and corresponding effective masses moves down in energy. At the values assumed in the dispersion calculation (see the caption to Figure 2), we obtain the following values of dimensionless effective masses $m^*_{\mathrm{AB}} = m^1_{\mathrm{AB}}/m_e \approx 0.94$ and band parameters $E_g = 2$, $W = \sqrt{\Delta^2 + 4t^2} - \Delta \approx 1.24$. For the hypothetical AB_2 structure representing an AB biatomic chain, where each atom A is decorated by atom B, we have

$$m^1_{\mathrm{AB}_2} = -m^2_{\mathrm{AB}_2} = \frac{\hbar^2\sqrt{\Delta^2 + t_\perp^2}}{4t^2a^2},$$

so at the values assumed in the dispersion calculation, for dimensionless effective masses, we deduce

$$m^2_{\mathrm{AB}_2} = m^1_{\mathrm{AB}_2}/m_e \approx 1.06,$$

$$E_g = 2\sqrt{1.25} \approx 2.24, \quad W = \sqrt{\Delta^2 + t_\perp^2 + 4t^2} - \Delta \approx 1.17.$$

For ABC structure, we deduce

$$m^2_{\mathrm{ABC}} = \frac{3}{2f_1}\frac{\hbar^2 R_\perp}{4t^2a^2}, \quad m^{2,3}_{\mathrm{ABC}} = -\frac{\sqrt{3}}{f_{2,3}}\frac{\hbar^2 R_\perp}{4t^2a^2},$$

where, for the values assumed in the band calculation, $f_1 = 1.75$, $f_2 = 2.31$, $f_3 = -0.33$, so the listed effective masses are, respectively, equal to

$$m^*_{\mathrm{ABC},1} = m^1_{\mathrm{ABC}}/m_e \approx 1.14,$$

$$m^*_{\mathrm{ABC},2} = m^2_{\mathrm{ABC}}/m_e \approx -1.00,$$

$$m^*_{\mathrm{ABC},3} = m^3_{\mathrm{ABC}}/m_e \approx 6.99.$$

For band widths, we obtain $W_1 \approx 0.92$, $W_2 \approx 1.35$, $W_3 \approx 0.44$, $W_i = |y_i(0) - y_i(\pi/2)|$. For direct interband gaps we have

$$\Delta_\uparrow = \omega_1(\pi/2a) - \omega_3(\pi/2a) = 2.33,$$

$$\Delta_\downarrow = \omega_3(\pi/2a) - \omega_2(\pi/2a) = 0.41,$$

and for an indirect gap we obtain

$$\Delta_{\mathrm{indir}} = \omega_1(\pi/2a) - \omega_3(0) = 1.79.$$

Regarding carbynes [15], for cumulene and polyyne we have, respectively

$$\omega_{\mathrm{cum}}(k) = -2t\cos(ka), \quad |k_{\mathrm{cum}}| \le \pi/a,$$

$$\omega^{\pm}_{\mathrm{pol}}(k) = \pm R(k), \quad R(k) = 2t'\sqrt{A_1^2(k) + A_2^2(k)}, \qquad (7)$$

where $|k_{\mathrm{pol}}| \le \pi/2a$. By projecting $\omega_{\mathrm{cum}}(k)$ into the Brillouin zone of polyyne, we obtain the dispersion law written as

$$\omega^{\pm}_{\mathrm{cum}}(k) = \pm 2t\cos(ka), \quad |k_{\mathrm{cum}}| \le \pi/2a. \qquad (8)$$

Due to smallness of the relations ($\Delta a/a \approx -0.03$ and $\Delta t/2t \approx 0.03$: for more details,see [15]), significant differences in spectra (7) and (8) are observed only at $|k| \to \pi/2a$, where polyyne at $|k| = \pi/2a$ in the electronic spectrum has a gap $\Delta_{\mathrm{pol}} = 2R(\pi/2a) = 2\Delta t \approx 0.32$ eV (this value is in good agreement with findings obtained by other authors, see [15]), and cumulene has no gap. It is interesting to compare cumulene with zero-gap graphene and polyyne with gapped graphene. Then, at the Brillouin zone edge of cumulene (i. e. equivalent of the Dirac point of graphene), spectrum (9) may be described by the Fermy velocities

$$v_F^{1D} = \mp 2ta/\hbar \sim 10^6 \text{ m/s} \qquad (9)$$

(estimate for π-bands, see [15]), i.e. the same result as for graphene. Effective masses $(m^{\pm}_{\mathrm{cum}})^* = \hbar^2/m_e 2ta^2 \approx 0.8$ may be introduced into the center of the Brillouin zone of cumulene.

Let us now compare the spectra of polyyne and AB structure. For cumulene with the dispersion law $\omega_{\mathrm{cum}}(k) = -2t\cos(ka)$, we obtain (per a spin projection)

$$\rho_{\mathrm{cum}}(\omega) = \begin{cases} \dfrac{1}{\pi\sqrt{4t^2 - \omega^2}}, & \omega^2 \le 4t^2, \\ 0, & \omega^2 > 4t^2. \end{cases} \qquad (10)$$

For dispersion $\omega^{\pm}_{\rm cum}(k) = \pm 2t\cos(ka)$ we have

$$\rho^{\pm}_{\rm cum}(\omega) = \begin{cases} \dfrac{\pi/2 \mp \arcsin(\omega^2/4t^2)}{\pi\sqrt{4t^2-\omega^2}}, & \omega^2 \le 4t^2, \\ 0, & \omega^2 > 4t^2. \end{cases} \quad (11)$$

Let us now proceed to examination of the densities of states for AB, AB_2 and ABC structures. For AB structure with spectrum

$$\omega_{\pm}(k) = \bar{\varepsilon} \pm \sqrt{(\Delta^2 + 2t^2) + 2t^2\cos(2ka)},$$

where $\bar{\varepsilon} = (\varepsilon_a + \varepsilon_b)/2$, $\Delta = |\varepsilon_a - \varepsilon_b|/2$, $\Omega = \omega - \bar{\varepsilon}$, the density of states is equal to

$$\rho_{\rm AB}(\Omega) = \begin{cases} \dfrac{1}{\pi}\dfrac{|\Omega|}{\sqrt{(W^2_{\rm top}-\Omega^2)(\Omega^2-W^2_{\rm bot})}}, \\ \quad \Delta^2 = W^2_{\rm bot} \le W^2_{\rm top} = \Omega^2 \le \Delta^2 + 4t^2, \\ 0, \quad \Omega^2 < \Delta^2, \ \ \Omega^2 > \Delta^2 + 4t^2, \end{cases} \quad (12)$$

where $W_{\rm top(bot)}$ means the top(bottom) boundary of the continuous spectrum. For AB_2 structure with spectrum $\omega_{\pm}(k) = \bar{\varepsilon} \pm R(k)$ and $\omega_0 = 0$, where

$$R(k) = \sqrt{\Delta^2_{\perp} + 4t^2\cos^2(ka)},$$

$$\Delta_{\perp} = \sqrt{\Delta^2 + t^2_{\perp}}, \quad \Omega = \omega - \varepsilon_a/2$$

densities of states are written as $\rho^{(3)}_{\rm AB_2}(\omega) = \delta(\omega)$,

$$\rho^{(1,2)}_{\rm AB_2}(\Omega) = \begin{cases} \dfrac{1}{\pi}\dfrac{|\Omega|}{\sqrt{(W^2_{\rm top}-\Omega^2)(\Omega^2-W^2_{\rm bot})}}, \\ \quad \Delta^2_{\perp} = W^2_{\rm bot} \le \Omega^2 \le W^2_{\rm top} = \Delta^2_{\perp} + 4t^2, \\ 0, \quad \Omega^2 < \Delta^2_{\perp}, \ \ \Omega^2 > \Delta^2_{\perp} + 4t^2. \end{cases} \quad (13)$$

For ABC structure, densities of states for bands 1 and 2 are written as

$$\rho^{(1,2)}_{\rm ABC}(\omega) = \begin{cases} \dfrac{1}{\pi}\dfrac{|\omega|}{\sqrt{(W^2_{\rm top}-\omega^2)(\omega^2-W^2_{\rm bot})}}, \\ \quad W^2_{\rm bot} = \varepsilon_{\perp} \le \omega^2 \le W^2_{\rm top} = \varepsilon^2_{\perp} + 4t^2, \\ 0, \quad \omega^2 < \varepsilon^2_{\perp}, \ \ \omega^2 > \varepsilon^2_{\perp} + 4t^2. \end{cases} \quad (14)$$

It could be shown that for band 3 at $t^2_{\perp}/\varepsilon^2 \ll 1$ we approximately obtain

$$\rho^{(3)}_{\rm ABC}(\omega) \approx \begin{cases} \dfrac{1}{\pi}\dfrac{\omega^2}{\sqrt{W_{\rm top} - |\omega|}\sqrt{|\omega| - W_{\rm bot}}}, \\ \quad W_{\rm bot} \le |\omega| \le W_{\rm top}, \\ 0, \quad |\omega| < W_{\rm bot}, \quad |\omega| > W_{\rm top}, \end{cases} \quad (15)$$

i.e. an expression similar to (10), see also, for example, equations (10) and (12) in [40], that discussed a quasi-one-dimensional structure — adparticle-decorated zigzag edge of graphene nanoribbon. It should be noted that densities of states (8)–(10) with root features are typical for 1D systems [43] (the same is applicable to equations (10) and (12) in [41]).

2.2. Carbyne conductance

Let us start from the most extensively studied quantum transport in carbynes. The first (according to the authors) conductance measurements on the monoatomic chain of carbon atoms were performed in [44]. The chains were obtained by removal of atoms from a carbon nanoribbon that carried electric current. Formation of chains was followed by a typical drop of conductivity. Conductance of chains appeared to be much lower than the expected conductance of ideal chains. Ab initio calculations have shown that the effect of mechanical stresses in chains on conductance increases as the chain length grows. These stresses may also cause cumulene transition to polyyne, i.e. metal–semiconductor transition. According to [44], cumulene demonstrates quantum conductance $2G_0$, where conductance quantum $G_0 = 2e^2/h$ (e is the elementary charge, h is Planck's constant) conductance of one channel in the ballistic transport (multiplier 2 occurs due to the presence of doubly-degenerate π-bands formed by p_z and p_y orbitals (the chain is extended along the $\hat{x}$ axis), that corresponds to $0.15\,\mu$A at the bias voltage $V_b = 0.1$ V. Gap widths in the polyyne spectrum equal to 0.38 and 0.34 eV are also provided there. Similar results were obtained in [45], where transport properties of carbon wire „stretched" between two graphene electrodes were addressed. Conductance of insulated wire was found to be equal to $1.06G_0$, and for twin wire $1.47G_0$ that is lower than $2G_0$ due to overlapping of wave functions of adjacent wire atoms. Calculations in [44,45] used the method of Green's function together with DFT (density functional theory) [46] and the Landauer formula (see [43], Ch. 5), according to which the current-voltage curve I–V is defined as follows

$$I = G_0 \int T(\omega, V_b)[f_L(\omega) - f_R(\omega)]d\omega,$$

where $f_{L(R)}$ are the fermionic distribution functions on the left (right) electrode, $T(\omega, V_b)$ is the transmission ratio [47] at ω and V_b. Note also [48] where conductance of short polyyne nanochains was calculated also within the Landauer formalism. Such objects of study are selected because only relatively short chains, e.g. polyyne containing 44 atoms, have been synthesized until recently, a super long 1D chain containing 6000 atoms integrated into a double-walled carbon nanotube (CNT) has been successfully created now [12,49]. When the chain length L is lower than relaxation lengths in momentum L_m and phase L_{φ}, the transport is known as coherent (only elastic scattering takes place), at $L \ll L_m, L_{\varphi}$ we have the ballistic condition; when $L \ge L_m, L_{\varphi}$, there is non-coherent transport characterized by inelastic scattering where electron-electron

and electron-phonon scattering shall be considered [50]. When interaction between carriers and the presence of diffuser in the transport channel are considered, the problem becomes more complicated [51].

2.3. Diffusion conductivity and thermoelectronic properties of free-standing 1D structures

Using the kinetic Boltzmann equation in a relaxation time approximation τ [52] and approach developed in [53–56] to the calculation of TE properties of 2D structures, we obtain the spectral conductance expression [52] written as

$$\sigma(\mu) = e^2\rho(\mu)v^2(\mu)\tau(\mu), \tag{16}$$

where μ is the chemical potential, e is the elementary charge, ρ is the density of states of cumulene (in eV^{-1}), v is the group velocity of electron (this expression, like the next equations in paragraph 2.3, are not applicable to the flat band $\omega_0 = \varepsilon_c = 0$ that shall be addressed in a special way [57]). To characterize thermoelectric properties, the thermoelectric power factor is often used $PF = \sigma S^2$, where S is the Seebeck coefficient equal to

$$S = C_S\big(d\ln\sigma(\mu, T=0)/d\mu\big), \quad C_S = -\pi^2 k_\mathrm{B}^2 T/3e, \tag{17}$$

k_B is the Boltzmann constant, T is the temperature. According to (9), for cumulene $v_\mathrm{cum} = 2ta/\hbar$ (for zero-gap graphene, we have $v_\mathrm{F}/\sqrt{2}$, where v_F is the Fermy velocity). Thus, for cumulene $S_\mathrm{cum}(\mu) = 0$ and $PF_\mathrm{cum}(\mu) = 0$. For polyyne, we obtain

$$v_\mathrm{pol}^2(\mu) = v_\mathrm{cum}^2\left(\frac{\mu^2 - \Delta_\mathrm{pol}^2}{\mu^2}\right), \quad \mu^2 > \Delta_\mathrm{pol}^2, \tag{18}$$

where $E_g = 2\Delta_\mathrm{pol} = 2\Delta t \approx 0.32\,\mathrm{eV}$ [15]. This expression is equivalent to equation (4) in [54] for the gapped graphene where, instead of v_cum^2 and Δ_pol^2, $v_\mathrm{F}^2/2$ and Δ^2 are used. By assuming $\tau(\mu) = C_\tau/\rho(\mu)$ [53–56], we obtain $\sigma(\mu) = e^2v^2(\mu)$. Then from (17) and (18) it follows that

$$S_\mathrm{pol}(\mu) = 2C_S\frac{\Delta_\mathrm{pol}^2}{\mu(\mu^2 - \Delta_\mathrm{pol}^2)},$$

$$PF_\mathrm{pol}(\mu) = 4C_S^2C_\tau e^2\frac{v_\mathrm{cum}^2\Delta_\mathrm{pol}^4}{\mu^4(\mu^2 - \Delta_\mathrm{pol}^2)}. \tag{19}$$

Thus, at $\mu \to \pm\Delta_\mathrm{pol}$, $S_\mathrm{pol}(\mu)$ and $PF_\mathrm{pol}(\mu)$ have power divergences.

Proceeding to other 1D structures addressed in paragraph 2.1 and assuming that their diffusion conductivity is also described by expression (16), and the dispersion law is written as $\omega(k) = \pm\Delta \pm \hbar^2k^2/2m$, where $\pm$ are applicable, respectively, to the conduction band and valence band, m is the effective mass and energy is measured from the midgap $E_g = 2\Delta$, for group velocity $v(k) = \hbar k/m$ we obtain

$$v^2(\mu) = \frac{2(\mu \mp \Delta)}{m}, \quad \mu^2 > \Delta^2, \tag{20}$$

Then, at $\tau(\mu) = C_\tau/\rho(\mu)$, we get

$$S(\mu) = C_S\frac{1}{\mu \mp \Delta}, \quad PF(\mu) = 2C_S^2C_\tau e^2\frac{1}{m(\mu \mp \Delta)}. \tag{21}$$

Assuming $\tau(\mu) = \tau_0 = \mathrm{const}$ (see Appendix A in [54]), then

$$S(\mu) = C_S\left(\frac{d\ln v(\mu)}{d\mu} + \frac{d\ln\rho(\mu)}{d\mu}\right). \tag{22}$$

Thus, divergences associated with the density of states are added to the divergences associated with the group velocity. Since for cumulene, the first term in (22) is equal to zero, we obtain $S(\mu) = C_S/2(4t^2 - \mu^2)$. For other 1D structures examined herein, it can be easily shown that identical divergences of the Seebeck coefficient occur near the boundaries of the continuous spectrum W_top and W_bot. The same may be also said about the thermoelectric power factor.

3. Epitaxial 1D structures on *d*-metals

3.1. Experiment

A fact [58,59] of quite peculiar interaction between adatoms on faces with strongly anisotropic atomic profile such (112) face of BCC lattice and (110) face of FCC lattice (e.g. W (112), Mo (112), Re (1010)) has been established by the sciences of the Institute of Physics of NAS of Ukraine more than 30 years ago. These faces are built from parallel closely-packed rows of atoms separated by „grooves“ with atomic depth (see Figure 11 in [58] and Figures 9, 10 in [59]). On such surfaces, metal and non-metal atoms form structures of clearly pronounced one-dimensional nature. alkaline, alkaline-earth and rare-earth metals were used as adatoms. To form 1D chains of atoms with small coverage, attractive forces between adatoms in these chains must be present. Since the abovementioned metallic adsorbates feature significant polarity of adsorption bond, then quite strong dipole-dipole repulsion is present between adatoms [43]. Therefore, generation of chains suggests that direct and indirect exchange prevails in the interaction between adatoms [43]. Ch. 9). Thus, an attempt may be made to generate long carbyne chains on striated surfaces of *d*-metals. The same conclusion is suggested by the history of silicene that could not be synthezied in a free form, but whose nanoribbons were grown on (111) Ag surface in 2012 [60]. Stabilizing effect of metallic atoms on carbynes is also supported by calculations in [61,62]. The first of them investigates atomic structure and electron transport properties of the carbon chain with interstitial copper atoms (Cu-metallized carbyne) to prevent the Peierls transition of carbyne to polyyne; as a result, the Cu-mettalized carbyne behaves as a one-dimensional metal. Carbyne decoration by calcium atoms was discussed in [62]. In particular, it was shown that Ca atom is bonded more strongly with single C−C bond, rather than with triple C≡C bond. Due to deformation induced by Ca adsorption,

C−C and ≡C bond lengths become almost the same (1.29 and 1.30 Å, respectively).

On the other hand, it should be noted that one-dimensional structures were not found in the series of papers of Ioffe Institute sciences [63–68] that studied carbon coatings on d-metals (Ir (111) [64], Mo (100) [65], Ta (100) [66], Re [67], Pt (111) [68]). This should come as no surprise, since the crystal faces of d-metals used in experiments [63–68] have no striated structure.

3.2. Epitaxial chains on d-metals: theoretical estimations

To describe epistructures, use so-called adsorption approach [69], according to which, if Green's function of a free-standing structure is equal to $G(\omega)$, then Green's function of epistructure $\tilde{G}(\omega)$ is defined by the Dyson equation $\tilde{G}^{-1}(\omega) = G^{-1}(\omega) - \Sigma(\omega)$, where self-energy part $\Sigma(\omega) = \Lambda(\omega) - i\Gamma(\omega)$, and $\Lambda(\omega)$ and $\Gamma(\omega)$ are, respectively, energy level shift and broadening functions of a free structure as result of its interaction with the substrate. In this case $\Gamma(\omega) = \pi V^2 \rho_{\text{sub}}(\omega)$, where V is the matrix element of interaction between the epistructure and substrate, whose density of states is equal to ρ_{sub}, and $\Lambda(\omega)$ is the Hilbert transform function $\Gamma(\omega)$, i. e.

$$\Lambda(\omega) = \pi^{-1} P \int_{-\infty}^{\infty} \frac{\Gamma(\omega')d\omega'}{\omega - \omega'},$$

where P is the symbol of the main value. For the following analysis, density of states of the substrate shall be set. Using the Friedel model, assume $\rho_{\text{sub}}(\omega) = \rho_d = 10/W_d$ at $-W_d/2 \le \Omega_d \le W_d/2$ and $\rho_{\text{sub}}(\omega) = 0$ in other cases, where $\Omega_d = \omega - E_d$, W_d is the conduction band width of d-metal with center E_d (see [39]. Ch. 20). broadening function $\Gamma_d(\omega) = \pi\rho_d(\omega)V^2$ and shift function

$$\Lambda_d(\omega) = \frac{\Gamma_d}{\pi} \ln\left|\frac{\Omega_d + W_d/2}{\Omega_d - W_d/2}\right|, \qquad (23)$$

where $\Gamma_d = \pi\rho_d V^2$. Now, in expressions (10)−(15) for densities of states of free 1D structures we shall replace ω with $\tilde{\omega} = \omega - \Lambda_d(\omega)$ and in expressions (18)−(22) for $v(\mu)$ and $\rho(\mu)$ we shall replace μ with $\tilde{\mu} = \mu - \Lambda_d(\mu)$, that of course shifts the poles. Here, for order of magnitude estimates, we assume a so-called wide band approximation, when $W_d \to \infty$ is assumed (for 5d-metals $W_d \sim 10$ eV), that gives $\Lambda_d(\omega) = 0$ [43, Ch. 8]. Let us now estimate charge Z_0 of a singe adatom, from which the epitaxial chain is built using the equation

$$Z_0 = \frac{2}{\pi} \arctan \frac{\varepsilon_a - E_{\text{F}}}{\Gamma_d}, \qquad (24)$$

where ε_a is the energy of orbital that acts in adsorption and is initially filled by one electron, E_{F} is the Fermi energy [43, Ch. 8]. Implying the carbon adatom, replace $\varepsilon_a - E_{\text{F}}$ with work function difference of carbon structures and d-metal $\varphi_C - \varphi_d$. Such procedure is possible because graphene and graphite have the same work functions $\varphi_C = 4.50$ eV [70], work functions of the monolayer and double-layer graphene also have a little difference [71]. Therefore, for estimates, we assume $\varphi_C = 4.50$ eV also for the carbon chain. For Mo (112) $\varphi_d = 4.36 - 4.53$ [72], for W (112) $\varphi_d \approx 4.7$ eV [73,74]. According to [39] (Ch. 19), the matrix element that binds p-states of carbon with d-states of metal substrate $V = V_{pd\sigma} = 2.95(\hbar^2 r_d^{3/2}/md^{7/2})$ for σ-bond, r_d is the radius of d-shell equal to (1.27 and 1.20 Å) for W and Mo, respectively. Assuming the adsorption bond length $d \sim 2.5$ Å, we get $V_{pd\sigma} \sim 1$ eV, so $\Gamma_d \sim 3$ eV (for σ-bond). Then from (24) it follows that $|Z_0| \ll 1$. Providing that carbon atoms in the chain are bonded through direct exchange t and are spaced at a, then the chain is stable, when the Coulomb repulsion energy of adjacent adatoms $U_C = \frac{Z_a^2 e^2}{a}$ is lower than their bond energy $U_{\text{bind}} = 2t/3$, where $t = \eta_{sp}(\hbar^2/ma^2)$ and for σ-bond of sp-orbitals $\eta_{sp} = 3.19$ [76], hence, we obtain $Z_0^2 < 1/a$, where a is measured in Å. The same chain stability condition may be also written for indirect interaction of adjacent adatoms ([43], Ch. 9).

In addition, consider the effect of electron-electron repulsion of adjacent atoms in the chain $Gn_j n_{j\pm1}$, where $n_J \sim 1$, because $|Z_j| \ll 1$, where j is the atom number in the chain. Ch. 9 [43] and [77] show that in certain conditions of a chain with uniform distribution of electrons over atoms it is favorable to change to a state with a charge-density wave due to interatomic transfer of electrons, when the occupation numbers of adjacent atoms are $n_j = 1 + \delta n$, $n_{j\pm1} = 1 - \delta n$, so attraction occurs between them that reduces the chain energy by $G(\delta n)^2$. While the chain stability certainly increases.

It should be also noted that when the dipole-dipole repulsion in chain and in other structures is considered (dipoles are formed by adatoms and their images in metal), depolarization of adatoms takes place, i. e. decrease of charge of adatoms ([43], Ch. 9).

3.3. Estimation of thermoelectric properties of epitaxial chains

For the epitaxial cumulene, the density of states

$$\tilde{\rho}(\omega) = \frac{\Gamma}{\pi} \int_0^{\pi/2} \frac{d(ka)}{\left(\omega - 2t\cos(ka)\right)^2 + \Gamma^2}, \qquad (25)$$

hence, the maximum value is $\tilde{\rho}_{\text{cum}} = 1/\pi\Gamma$ (it can be shown that

$$\tilde{\rho}_{\text{cum}}(0) = (4t^2 + \Gamma^2)^{-1/2}$$

and

$$\rho_{\text{cum}}(\pm 2t) \sim \Gamma/\pi(4t^2 + \Gamma^2).$$

Thus, divergences of conductance (16) and thermoelectronic properties $S_{\text{cum}}(\mu)$ and $PF_{\text{cum}}(\mu)$ associated with the

features of densities of states in relaxation time approximation by constant (the second term in expression (22)), are absent in epistructures on d-metals in a wide band approximation. However, features associated with group velocity (18), (20), (22) are still exhibited. Therefore, the effect of substrate on the group velocity determined for the first time for graphene in [78] and for carbyne in [77] shall be considered. According to these papers

$$\tilde{v}(\mu)/v(\mu) = F(\mu), \quad F(\mu) = \left(1 - \left(d\Lambda(\mu)/d\mu\right)\right)^{-1}. \quad (26)$$

Thus, in a wide band approximation, we have $\tilde{v}(\mu)/v(\mu) = 1$. While in the Friedel model from (23) we obtain

$$F(\mu) = \left(1 + \frac{\Gamma_d}{\pi} \frac{W_d}{(W_d/2)^2 - (\mu - E_d)^2}\right)^{-1}. \quad (27)$$

Relations of effective masses for epitaxial and free structures $\tilde{m}^*/m^* = F(\omega_{\text{extr}})$, where ω_{extr} is the energy of extremum for which effective masses were determined. More detailed discussions of dependences (26), (27) (in particular, threshold $\mu \to E_d \pm W_d/2$) are described in [78,77].

From equations (19) and (26) it follows that for cumulene, polyyne and other 1D structures addressed herein, the following relations are valid

$$\tilde{S}(\mu)/S(\mu) = 1 \text{ and } \left(PF(\mu)\right)_{\text{epi}}/\left(PF(\mu)\right)_{\text{free}} = F^2(\mu). \quad (28)$$

4. Conclusion

This study uses the tight-binding approximation and Green's functions to derive analytical expressions for electronic spectrum properties (dispersion and effective carrier masses) for five one-dimensional free structures and to show that densities of states of all given structures ρ are characterized by root divergence when the chemical potential approaches the continuous spectrum boundaries of these structures. Assuming that relaxation time $\tau \propto \rho^{-1}$, spectral conductance $\sigma(\mu) \propto v^2(\mu)$, where v is the group velocity of electron (such proportion is specific to the kinetic Boltzmann equation), simple analytical expressions were obtained for the Seebeck coefficient $S(\mu)$ and thermoelectric power factor $PF(\mu)$ of free 1D structures.

Transition to epitaxial structures is preceded by a summary of the available experimental data on generation of chains on striated faces of transition metals. Simple theoretical estimates have shown that such chains built from carbon atoms (i.e. carbines) shall be stable. It has been also shown that the presence of d-substrate changes ρ, v, s and PF.

Interest in extreme values of thermoelectric properties is induced by search for materials and structures having $ZT > 1$ (known as figure of merit in English literature), where $Z = \sigma S^2/\kappa$, κ is the heat capacity [79].

Conflict of interest

The author declares that he has no conflict of interest.

References

[1] A.K. Geim, K.S. Novoselov. Nature Mater. **6**, 183 (2007).
[2] A.K. Geim, I.V. Grigorieva. Nature **499**, 419 (2013).
[3] C.-J. Tong, H. Zhang, Y.-N. Zhang, H. Liu, L.-M. Liu. J. Mater. Chem. A **2**, 17971 (2014).
[4] S. Haastrup, M. Strange, M. Pandey, T. Deilmann, P.S Schmidt, N.F. Hinsche, M.N. Gjerding, D. Torelli, P.M. Larsen, A.C. Riis-Jensen, J. Gath, K.W. Jacobsen, J.J. Mortensen, T. Olsen, K.S. Thygesen. 2D Mater. **5**, 042002 (2018).
[5] L. Vannucci, U. Petralanda, A. Rasmussen, T. Olsen, K.S. Thygesen. J. Appl. Phys. **128**, 105101 (2020).
[6] M. Fukuda, J. Zhang, Y.-T. Lee, T. Ozakia. Mater. Adv. **2**, 4392 (2021).
[7] N. Briggs, S. Subramanian, Z. Lin, X. Li, X. Zhang, K. Zhang, K. Xiao, D. Geohegan, R. Wallace, L.-Q. Chen, M. Terrones, A. Ebrahimi, S. Das, J. Redwing, C. Hinkle, K. Momeni, A. van Duin, V. Crespi, S. Kar, J.A. Robinson. 2D Mater. **6**, 022001 (2019).
[8] J. Nevalaita, P. Koskinen. Phys. Rev. B **97**, 035411 (2018).
[9] Yu.P. Kudryavtsev, R.B. Heimann, S.E. Evsyukov. J. Mater. Sci. **31**, 5557 (1998).
[10] F. Banhart. Belstein J. Nanotechnol, **6**, 559 (2015).
[11] L. Shi, P. Rohringer, K. Suenaga, Y. Niimi, J. Kotakoski, J.C. Meyer, H. Peterlik, M. Wanko, S. Cahangirov, A. Rubio, Z.J. Lapin, L. Novotny, P. Ayala, T. Pichler. Nature Mater. **15**, 634 (2016).
[12] L. Shi, P. Rohringer, M. Wanko, A. Rubio, S. Waserroth, S. Reich, S. Cambre, W. Wenseleers, P. Ayala, T. Pichler. Phys. Rev. Mater. **1**, 075601 (2017).
[13] Z. Salman, A. Nair, S. Tung. Proc. 12th IEEE Int. Conf. on Nano/Micro Engineered and Molecular Systems (April 9–12, 2017) Los Angeles, USA. P. 667–681.
[14] C.S. Casar, A. Milani. MRS Commun. **8**, 207 (2018).
[15] S.Yu. Davydov. Semiconductors **53**, 954 (2019).
[16] S. Gunasekaran, L. Venkataraman. J. Chem. Phys. **153**, 124304 (2020).
[17] M. Bamdad, H. Mousavi. ECS J. Solid State Sci. Technol. **10**, 031001 (2021).
[18] R.T. Senger, S. Tongay, E. Durgun, S. Ciraci. Phys. Rev. B **72**, 075419 (2005).
[19] H.L. Zhuang, A.K. Singh, R.G. Hennig. Phys. Rev. B **87**, 165415 (2013).
[20] C.-J. Tong, H. Zhang, Y.-N. Zhang, H. Liu, L.-M. Liu. J. Mater. Chem. A **2**, 17971 (2014).
[21] S.Yu. Davydov. Semiconductors **54**, 523 (2020).
[22] S.Yu. Davydov. Phys. Solid State **62**, 1085 (2020).
[23] S. Hasegawa. J. Phys.: Condens. Matter **22**, 084026 (2010).
[24] P.D. Bhuyan, S.K. Gupta, Y. Sonvane, A. Kumar. AIP Conf. Proceed. **1942**, 110026 (2018).
[25] P.B. Sorokin, H. Lee, L.Yu. Antipina, A.K. Singh, B.I. Yakobson. Nano Lett. **11**, 2660–2665 (2011).
[26] X. Tu, H. Wang, Z. Shen, Y. Wang, S. Sanvito, S. Hou. J. Chem. Phys. **145**, 244702 (2016).

[27] Z. Salman, A. Nair, S. Tung. Proc. 12th IEEE Intern. Conf. Nano/Micro Engineered and Molecular Systems Los Angeles, USA (2027). p. 677.
[28] A.P. Piedade, L. Cangueiro. Nanomaterials **10**, 780 (2020).
[29] A. Machín, K. Fontánez, J.C. Arango, D. Ortiz, J. De León, S. Pinilla, V. Nicolosi, F.I. Petrescu, C. Morant, F. Márquez. Materials **14**, 2609 (2021).
[30] M. Aleksandrova, G. Kolev, A. Brigadin, A. Lukin. Crystals **12**, 501 (2022).
[31] M. Ashton, J. Paul, S.B. Sinnott, R.G. Hennig. Phys. Rev. Lett. **118**, 106101 (2017).
[32] M. Fukuda, J. Zhang, Y.-T. Lee, T. Ozakia. Mater. Adv. **2**, 4392 (2021).
[33] S.V. Demisheva, A.A. Pronina, V.V. Glushkova, N.E. Sluchanko, N.A. Samarina, M.V. Kondrinb, A.G. Lyapin, V.V. Brazhkinb, T.D. Varfolomeeva, S.V. Popova. JETPh **95**, 123 (2020).
[34] A.M. Dehkordi, M. Zebarjadi, J. He, T. M. Tritt. Mater. Sci. Eng. R **97**, 1 (2015).
[35] D. Li, Y. Gong, Y. Chen, J. Lin, Q. Khan, Y. Zhang, Y. Li, H. Zhang, H. Xie. Nano-Micro Lett. **12**, 36 (2020).
[36] N.T. Hung, A.R.T. Nugraha, R. Saito. Phys. Rev. Appl. **9**, 024019 (2018).
[37] E.H. Hasdeo, L.P.A. Krisna, M.Y. Hanna, B.E. Gunara, N.T. Hung, A.R. Nugraha. J. Appl. Phys. **126**, 035109 (2019).
[38] A. Darmawan, E. Suprayoga, A.R.T. Nugraha, A.A. AlShaikhi. arXiv: 2205.10603.
[39] W. Harrison, Elektronnaya struktura i svoistva tverdykh tel. Mir, M. (1983). (in Russian).
[40] W.A. Harrison. Phys. Rev. B **31**, 2121 (1985).
[41] S.Yu. Davydov. Semiconductors **53**, 78 (2019).
[42] S.Yu. Davydov. Phys. Solid State **61**, 480 (2019).
[43] S.Yu. Davydov, A.A. Lebedev, O.V. Posrednik. Elementarnoye vvedeniye v teoriyu nanosistem. Lan', SPb (2014). Gl. 2. (in Russian).
[44] O. Cretu, A.R. Botello-Mendez, I.M. Janowska, C. Pham-Huu, J.-C. Charlier, F. Banhart. Nano Lett. **13**, 3482 (2013).
[45] L. Shen, M. Zeng, S.-W. Yang, C. Zhang, X. Wang, Y. Feng. J. Am. Chem. Soc. **132**, 11481 (2010).
[46] G. Onida, L. Reining, A. Rubio. Rev. Mod. Phys. **74**, 601 (2002).
[47] D.S. Fisher, P.A. Lee. Phys. Rev. B **23**, 6851 (1981).
[48] H. Mousavi, M. Bamdad, S. Jalilvand. ECS J. Solid State Sci. Technology **11**, 091003 (2022).
[49] L. Shi, P. Rohringer, K. Suenaga, Y. Niimi, J. Kotakoski, J.C. Meyer, H. Peterlik, M. Wanko, S. Cahangirov, A. Rubio, Z.J. Lapin, L. Novotny, P. Ayala, T. Pichler. Nature Mater. **15**, 634 (2016).
[50] W.Y. Kim, Y.C. Choi, S.K. Min, Y.C. K.S. Kim. Chem. Soc. Rev. **38**, 2319 (2009).
[51] V.V. Afonin. JETP **163**, N. 2 (2023).
[52] J. Zayman, Printsipy teorii tverdogo tela. Mir, M., (1974), Gl. 7. (in Russian).
[53] H. Usui, K. Kuroki. J. Appl. Phys. Phys. Rev. B **121**, 165101 (2017).
[54] E.H. Hasdeo, L.P.A. Krisna, M.Y. Hanna, B.E. Gunara, N.T. Hung, A.R.T. Nugraha. J. Appl. Phys. **126**, 035109 (2019).
[55] J.M. Adhidewata, A.R.T. Nugraha, E. H. Hasdeo, P. Estell, B.E. Gunara. arXiv: 2107.06826.
[56] A. Darmawan, E. Suprayoga, A.R.T. Nugraha, A.A. AlShaikhi. arXiv: 2205.10603.
[57] K.-E. Huhtinen, P. Törmä. arXiv: 2212.03192.
[58] L.A. Bol'shov, A.P. Napartovich, A.G. Naumovets, A.G. Fedorus. Usp. Fiz. Nauk **122**, 125 (1977).
[59] O.M. Braun, V.K. Medvedev. **157**, 631 (1989).
[60] G. Le Lay, D. Solonenko, P. Vogt. Synthesis of Silicene. In: Silicene. Nano-Science and Technology / Eds P. Vogt, G. Le Lay. Cham. Springer (2018). https://doi.org/10.1007/978-3-319-99964-7_5.
[61] P.B. Sorokin, H. Lee, L.Yu. Antipina, A.K. Singh, B.I. Yakobson. Nano Lett. **11**, 2660 (2011).
[62] X. Tu, H. Wang, Z. Shen, Y. Wang, S. Sanvito, S. Hou. J. Chem. Phys. **145**, 44702(2016).
[63] A.Ya. Tontegode. Prog. Surf. Sci. **38**, 201 (1991).
[64] A.Ya. Tontegode, E.V. Rut'kov. Usp. Fiz. Nauk **163**, 57 (1993).
[65] N.R. Gall, E.V. Rut'kov. JETP letters **71**, 671 (2000).
[66] N.R. Gall, E.V. Rut'kov, A.Ya. Tontegode. JETP Lett. **73**, 756 (2001).
[67] E.V. Rut'kov, N.R. Gall. JETP Lett. **110**, 683 (2019).
[68] E.V. Rut'kov, N.R. Gall. JETP Lett. **113**, 595 (2021).
[69] S.Yu. Davydov. Phys. Solid State **58**, 804 (2016).
[70] D. Niesner, T. Fauster. J. Phys.: Condens. Matter **26**, 393001 (2014).
[71] Y.-J. Yu, Y. Zhao, S. Ryu, L.E. Brus, K.S. Kim, P. Kim. Nanj Lett. **9**, 3430 (2009).
[72] Fizicheskiye velichiny. Spravochnik / Pod. red. I.S. Grigoriyeva, Ye.Z. Meylikhova. Energoatomizdat, M., (1991). (in Russian).
[73] S.A. Shakirova, I. Bayo. Tech. Phys. Lett. **33**, *7*, 567 (2007).
[74] S.A. Surma, J. Brona, A. Ciszewski. Mater. Sci. (Poland) **36**, 225 (2018).
[75] S.Yu. Davydov, O.V. Posrednik. Phys. Solid State **57**, 837 (2015).
[76] W.A. Harrison. Phys. Rev. B **27**, 3592 (1983).
[77] S.Yu. Davydov. Tech. Phys. Lett. **45**, 650 (2019).
[78] Z.Z. Alisultanov. Tech. Phys. Lett. **39**, 507 (2013).
[79] A.M. Dehkordi, M. Zebarjad, J. He, T.M. Tritt. Mater. Sci. Eng. R **97**, 1 (2015).

Translated by E.Ilinskaya